Journal of Hydrology, 120 (1990) 359–379
Elsevier Science Publishers B.V., Amsterdam — Printed in The Netherlands

[3]

WATER AND SOLUTE MOVEMENT IN A COARSE-TEXTURED WATER-REPELLENT FIELD SOIL

J.C. VAN DAM[1], J.M.H. HENDRICKX[2], H.C. VAN OMMEN[3], M.H. BANNINK[3], M.TH. VAN GENUCHTEN[4] and L.W. DEKKER [5]

[1]*Department of Hydraulics and Catchment Hydrology, Agricultural University, Wageningen (The Netherlands)*
[2]*International Institute of Land Reclamation and Improvement (ILRI), Wageningen (The Netherlands)*
[3]*Grontmij Ltd. Engineers and Consultants, De Bilt (The Netherlands)*
[4]*U.S. Salinity Laboratory, USDA-ARS, Riverside, CA. (U.S.A.)*
[5]*Winand Staring Centre for Integrated Land, Soil and Water Resources, Wageningen (The Netherlands)*

(Received July 19, 1989; accepted after revision February 4, 1990)

ABSTRACT

Van Dam, J.C., Hendrickx, J.M.H., van Ommen, H.C., Bannink, M.H., van Genuchten, M.Th. and Dekker, L.W., 1990. Water and solute movement in a coarse-textured water-repellent field soil. J. Hydrol., 120: 359–379.

Unstable water flow in water-repellent unsaturated soils can significantly affect the processes of infiltration and soil water redistribution. A field experiment was carried out to study the effect of water-repellency on water and bromide movement in a coarse-textured soil in the southwestern part of The Netherlands. The field data were analyzed using a relatively simple numerical model based on the standard Richards' equation for unsaturated water flow and the Fickian-based convection-dispersion equation for solute transport. Water-repellency was accounted for by multiplying the water content and the unsaturated hydraulic conductivity of the soil with F, a factor equal to the volumetric fraction of soil occupied by preferential flow paths resulting from the unstable flow process. The good comparison of simulated and measured bromide concentrations suggests that the model provides a viable method for simulating unstable water flow in water-repellent soils.

INTRODUCTION

Water-repellent field soils can be found in many parts of the world under a variety of climatic conditions (DeBano, 1981). For example, water drop penetration time (WDPT) tests by the Soil Survey Institute revealed more than 75% of the agricultural top soils in The Netherlands to be moderately to extremely water-repellent, whereas more than 95% of the top soils in nature reserves exhibit strong to extreme water repellency. Numerous laboratory and field studies have been conducted to investigate the physics of fluid flow in water-repellent soils (Albert and Köhn 1926; Jamison, 1945; Meeuwig, 1971; DeBano,

0022-1694/90/$03.50

1975, 1981; Letey et al., 1975; Hendrickx et al., 1988a.) These indicate that infiltration rates into water-repellent soils can be considerably lower than those into wettable soils, and that wetting patterns in water-repellent soils can be quite irregular and incomplete. The studies also suggest that water-repellency has its greatest effect in relatively dry soils. As a result of water-repellency, water often flows through these soils in preferential paths or 'fingers'. Fingers have also been observed when water percolates from a fine-textured into a coarse-textured layer, in the case of low rainfall intensity, or when the air pressure increases ahead of the infiltration front (Hillel, 1987). The fingering process was studied in the laboratory by Hill and Parlange (1972), White et al. (1977), and Diment and Watson (1985); and in the field by Starr et al. (1978). Theoretical analyses were attempted by Raats (1973), Philip (1975), Parlange and Hill (1976), Diment et al. (1982) and Diment and Watson (1983).

Recently, Hendrickx et al. (1988b) studied solute movement in a coarse-textured water-repellent field soil and found their soil to be more vulnerable to groundwater pollution than a similar wettable soil. They also found that the instability criteria derived by Raats (1973) correctly predicted the occurrence of the unstable wetting fronts in their soil.

The purpose of this study was to analyze the field experiments of Hendrickx et al. (1988b) using a relatively simple model describing water flow and solute transport in water-repellent soils. Attention is also given to the sensitivity of predicted concentrations to changes in soil hydraulic properties, soil layering and the dynamics of the flow regime.

FIELD TRACER EXPERIMENT AND LABORATORY METHODS

In order to assess the influence of water-repellency on water flow and solute transport, several field experiments were conducted. These involved application of a bromide solution to a field soil, subsequently leached by natural rainfall.

The experimental site was located near the village of Ouddorp in the south-western part of The Netherlands on a sandy soil of marine origin, classified as a Mesic Typic Psammaquent (de Bakker, 1979). Bromide tracer experiments were carried out on two adjacent fields, one with a water-repellent top layer and one with a wettable top layer (Hendrickx et al., 1988b). The wettable top layer was calcareous with 5% clay and 2% organic matter content, while the water-repellent top layer was not calcareous and contained only 3% clay and 1.5% organic matter. The higher clay content of the wettable soil resulted from clay amendments about 30 years ago. The water table of the two fields during the experiments fluctuated between depths of 0.4 and 1.2 m. In both fields three identical plots of 6 m $\times$ 2 m were prepared.

On 12 November 1986, 1.25 mm KBr solution (11 g KBr l^{-1}) was applied to the six field plots. The solution was sprayed on the soil surface from a boom with six nozzles (Teejet 11002) spaced 0.33 m apart. The spraying pressure was 0.2 MPa and spraying height 0.3 m. Speed of walking during spraying was about

$1\,m\,s^{-1}$. During spraying, samples were collected at twelve random locations along the borders of each plot to verify the amount and areal distribution of the applied bromide pulse. The soil itself was sampled 13, 35 and 57 days after spraying, at which times samples were collected from five locations in each plot. The soil was sampled using a hollow cylinder that was driven mechanically into the soil. After removing the cover from the cylinder, the soil column was continuously sampled at 8 cm intervals (4–84 cm depth) with steel core cylinders (230 cm^3). These were emptied in a plastic jar and dried at 60° C. Next, 200 ml water was added to each jar and, after shaking for one hour, bromide was extracted by filtering through a dense paper filter and also through a membrane filter having a pore size of 0.45 μm. The extract passed the Baker-10 SPE system: a C18 reversed phase to exclude non-polar organic matter which may disturb the analysis. Concentrations in the extract were determined using ion chromatography (Harmsen, 1986).

Water repellency was measured with the water drop penetration time (WDPT) test described by DeBano (1969) and Letey et al. (1975). With this method a waterdrop is placed on a smooth air-dry surface of a soil sample and the time needed to penetrate the soil is recorded. Theoretically, a soil with a water–solid angle $\geqslant 90°$ should support a water drop on its surface until it evaporates. If the angle is less, capillary forces will draw water into the soil. The WDPT time was recorded up to 3600 s on disturbed samples which were dried for several days at 60° C. After removing samples from the stove, WDPT tests were deferred at least two days to allow samples to equilibrate with ambient air humidity.

Soil water retention curves were determined in the laboratory with the hanging water column ($0 < pF < 2.2$). Unsaturated conductivity was measured with the crust test in the range $0 < pF < 1.8$. Additonal details of the field experiment are given by Hendrickx et al. (1988b).

THEORY

Numerical model

Data were analyzed in terms of a numerical model (WORM) simulating water and solute movement in a one-dimensional soil profile (van Genuchten, 1987). The model assumes that unsaturated water-flow in a rigid soil system can be described with the Richards' equation as follows:

$$C\frac{\partial h}{\partial t} = \frac{\partial}{\partial z}\left[K\left(\frac{\partial h}{\partial z} - 1\right)\right] \tag{1}$$

where h is the soil water pressure head [L], $C = d\theta/dh$ is the differential soil water capacity [L^{-1}], θ is the volumetric water content [L^3L^{-3}], K is the unsaturated hydraulic conductivity [LT^{-1}], z is distance below the soil surface [L], and t is time [T].

The numerical solution of eqn. (1) requires estimates of the soil water

retention curve, $\theta(h)$, and the unsaturated hydraulic conductivity curve, $K(h)$. These curves are described with the functions of van Genuchten (1980):

$$\theta(h) = \theta_r + \frac{\theta_s - \theta_r}{[1 + (\alpha|h|)^n]^m} \quad (2)$$

$$K(S_e) = K_s S_e^l [1 - (1 - S_e^{1/m})^m]^2 \quad (3)$$

where θ_r and θ_s are the residual and field-saturated (satiated) water contents, respectively, K_s is the field-saturated hydraulic conductivity [LT^{-1}], α and n are empirical shape factors, $m = 1 - 1/n$, l is a pore-connectivity factor [-] assumed to be 0.5 by Mualem (1976), and S_e is the degree of saturation [-]:

$$S_e = \frac{\theta - \theta_r}{\theta_s - \theta_r} \quad (4)$$

Solute transport is calculated using the classical Fickian-based convection-dispersion equation:

$$\frac{\partial(\theta Rc)}{\partial t} = \frac{\partial}{\partial z}(\theta D \frac{\partial c}{\partial z} - qc) \quad (5)$$

where c is the solution concentration [ML^{-3}], R is the retardation factor [-], D is the dispersion coefficient [L^2T^{-1}], and q is the soil water flux density [LT^{-1}]:

$$q = -K\frac{\partial h}{\partial z} + K \quad (6)$$

The retardation factor, R, in eqn. (5) accounts for linear equilibrium sorption/exchange and is given by:

$$R = 1 + \rho k/\theta \quad (7)$$

where ρ is the soil bulk density [ML^{-3}] and k an empirical distribution coefficient [L^3M^{-1}].

The dispersion coefficient, D, in eqn. (5) represents the effects of both molecular diffusion and mechanical dispersion. As the net precipitation rate from November until March in The Netherlands averages about 2 mm day^{-1}, the effect of mechanical dispersion dominates the effect of molecular diffusion (Bolt, 1982). Therefore we assumed that D was adequately defined by:

$$D = \lambda|v| \quad (8)$$

where λ is the dispersivity [L], and v ($= q/\theta$) is the average pore-water velocity [LT^{-1}].

Equations (1) and (5) are solved in the WORM program using the relatively standard Galerkin linear finite element method with mass-lumping of the time derivatives (van Genuchten, 1982, 1987). The soil profile was assumed to be layered; each layer requiring its own hydraulic properties and transport parameters. The partial differential equations were solved subject to time-

dependent flux-type boundary conditions at the soil surface given by actual rainfall rates. Actual water table depths were prescribed by similarly invoking time-dependent pressure-head boundary conditions at the lower end of the soil profile.

Simulation of preferential flow paths

Hendrickx et al.(1988b) found that unstable wetting fronts at our study site caused irregular and incomplete wetting of the soil profile, indicating that only part of the soil matrix actively participated in the flow process. Because the WORM code considers the individual soil layers to be homogeneous horizontally, the model was modified by incorporating the macroscopic effects of preferential flow paths in the system. Germann (1988) discussed the restrictions imposed by convective-dispersive approaches and reviewed emerging alternate approaches. Among these are the consideration of mobile and immobile phases as applied by de Smedt and Wierenga (1979), the routing procedures along presumed stream lines and the transfer function models as introduced by Jury (1982).

The objective was to simulate water contents and bromide concentrations as functions of time and depth for transient flow conditions using soil hydraulic properties corrected for a part of the soil matrix not directly contributing to the flow process.

Assume that $\theta(h)$ and $K(S_e)$ are the microscopic retention and hydraulic conductivity functions of the preferential flow paths, while the stagnant parts are represented by stones with $\theta = 0$. If the hydraulic properties of the overall soil, including the stagnant parts, are measured in a large lysimeter it follows directly that:

$$\theta^*(h) = F\,\theta(h) \tag{9}$$

$$K^*(S_e) = F\,K(S_e) \tag{10}$$

where $\theta^*(h)$ and $K^*(S_e)$ are the apparent (macroscopic) water retention and hydraulic conductivity functions of the entire soil, while F represents the volumetric fraction of soil occupied by preferential flow paths. Because eqn. (9) does not affect the degree of saturation, S_e, and hence the hydraulic conductivity $K(S_e)$ as given by eqn. (3), the above modifications can easily be incorporated into the model. The depth-dependent coefficient F may be estimated by visual observation of wet and dry spots in the field, or by means of an iodide colour test (Hendrickx et al., 1988a; van Ommen et al. 1989b). Laboratory experiments by Glass et al. (1988) showed that preferential flow paths, once formed, persist from one infiltration cycle to the next. This might indicate that the volume of preferential flow paths is relatively stable during a season, which is a prerequisite for the use of F as a constant parameter.

Goodness of fit

The goodness of fit between calculated and measured water contents will be expressed in terms of the relative efficiency, RE (McCuen and Snyder, 1986), which is a measure of the improvement of the adopted model relative to the "zero" model which gives only the average concentration X_g of the entire profile:

$$RE = \frac{F_0 - F_1}{F_0} \times 100\% \tag{11}$$

where

$$F_0 = \sum_p (X_i - X_g)^2 \tag{12}$$

$$F_1 = \sum_p (X_i - X_c)^2 \tag{13}$$

where X_g is the arithmetic mean of all X_i observations, X_c is the calculated value corresponding to each X_i, and p is the total number of observations.

RE is a linear function of F_1. When $RE = 100\%$ ($F_1 = 0$), the simulation results duplicate exactly the measurements. When $RE = 0\%$ ($F_1 = F_0$), the simulation produces the same sum of squared deviations as when the predicted concentration equalled X_g. When RE is negative, the simulation is even worse.

DATA ANALYSIS

First the measured data (soil water content, WDPT test, bromide concentration, soil hydraulic properties) are discussed. Next attention is paid to the numerical simulation of the water flow. Finally the simulation of the bromide concentrations is shown.

Soil water content, WDPT *test, and bromide concentration*

Table 1 gives the total effective precipitation since the start of the field experiment on 12 November 1986, and also lists observed fluctuations of the water table during the experiment. Mean soil water contents at selected dates during the experiment are shown in Fig. 1. Results indicate that water contents steadily increased during the study period. The surface soil of the water-repellent soil contained ~5% less water than the surface soil of the wettable soil. Hendrickx et al. (1988b) give an extended analysis of the measured water contents.

Table 2 contains the results of the WDPT test. A soil is generally considered to be at least initially water repellent if a water drop is not absorbed within 5 s, WDPT values above 600 s are indicative of extreme water-repellency (DeBano, 1981; Richardson, 1984). McGhie and Posner (1980) consider WDPT values

TABLE 1

Effective precipitation, water table depths, and bromide recovery rates at selected sampling dates

Sampling date	Effective precipitation (mm)	Depth to groundwater (m)		Recovery rate (%)	
		Wettable soil	Water-repellent soil	Wettable soil	Water-repellent soil
25 Nov. 1986	61.8	0.83	0.73	70.3	91.3
17 Dec. 1986	93.3	0.78	0.68	70.0	97.6
8 Jan 1987	184.0	0.57	0.50	70.8	68.5

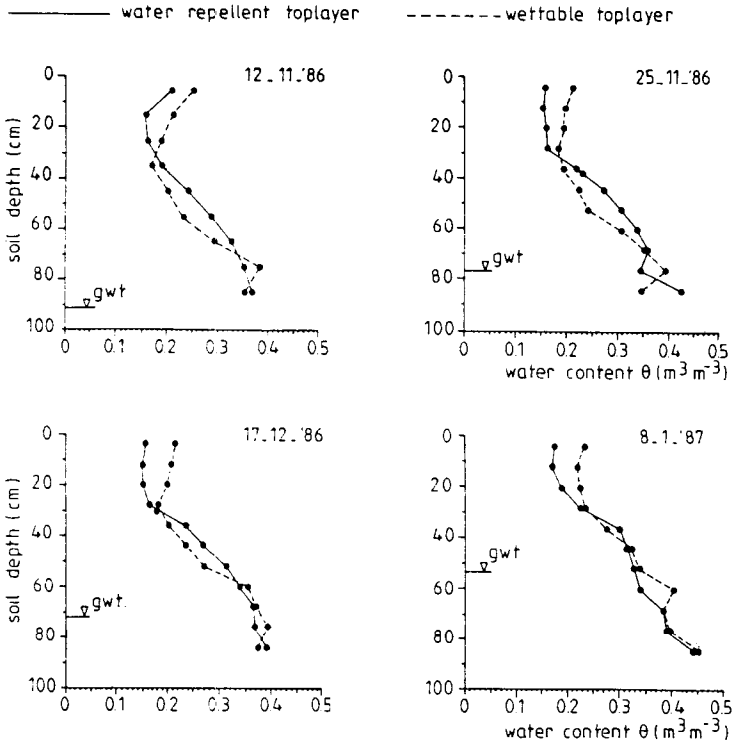

Fig. 1. Measured mean soil water contents in the wettable and water-repellent soils on four sampling dates.

above 60 s to be indicative of a stable water-repellent soil. These criteria suggest that the water-repellent top layers between depths of 0–0.1 and 0.1–0.3 m at our study site are extremely water-repellent and water-repellent, respectively. The wettable top layer at a depth of 0–0.1 m also appears to be water-repellent but this situation is not likely to persist. Because clay amendments were added only to the top soil, a few locations showed water-

TABLE 2

Water drop penetration time (WDPT) values (in s) for the wettable and water-repellent soils for four sampling dates. Each WDPT value is the mean of 15 values

Depth (cm)	Wettable soil				Water-repellent soil			
	A	B	C	D	A	B	C	D
0–10	22	100	31	163	842	1517	897	1071
10–20	1	1	1	1	35	224	48	252
20–30	1	1	1	1	4	229	2	17
30–40	1	7	422	24	1	1	1	1
40–50	40	56	748	107	1	1	1	1
50–60	1	12	104	17	1	1	1	1

A = 20/11/86, B = 25/11/86, C = 17/12/86, D = 08/01/87.

repellency below a depth of 0.3 m. The water-repellency of soil layers in this region (as observed in the laboratory) did not affect water flow because water repellency generally disappears under wet conditions (Letey et al., 1975; DeBano, 1981); soil water contents at these depths were always greater than 0.18.

Figure 2 shows the mean bromide concentrations measured on the three sampling dates. Observed peak concentrations in the water-repellent soil were less than those in the wettable soil. The bromide tracer also reached the groundwater table earlier in the water-repellent soil as compared with the wettable soil. After 62 mm rain, solutes in the wettable soil had reached a depth of 60 cm, whereas in the water-repellent soil a mean concentration of $\sim 20\,mg\,l^{-1}$ was measured in the groundwater at a depth of 80 cm. At the same time some of the bromide remained close to the soil surface of the water-repellent soil. Bromide recovery percentages for the two soils are listed in Table 1. Recovery percentages were always $< 100\%$, especially for the wettable soil, indicating some loss of bromide from the system, either in groundwater or perhaps because of some bromide uptake by the grass cover, which was more developed on the wettable soil.

Soil hydraulic properties

Figures 3 and 4 show the laboratory-measured water retention and hydraulic conductivity curves, respectively. The hydraulic properties of the water-repellent and wettable soils differ mainly in the surface layers, especially the wetting branches. This is particularly true near saturation where water contents of the water-repellent soil are 2–8% lower than those of the wettable soil. The parameters of van Genuchten's hydraulic functions (eqns (2) and (3)) were estimated by means of a least-square optimization analysis of the original laboratory data. Results are listed in Table 3. Parameter α for the wetting curve is always much higher than α for the drying curve indicating the presence of

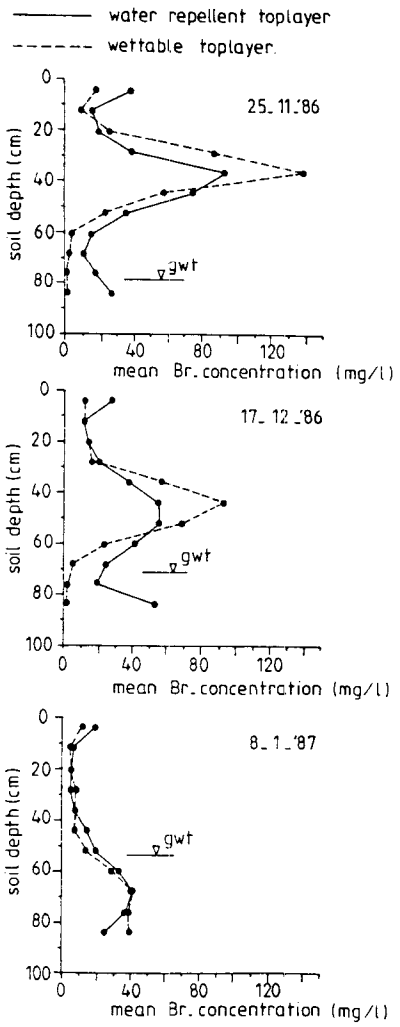

Fig. 2. Measured mean bromide concentrations in the wettable and water-repellent soils on three sampling dates.

hysteresis in the retention curve. Also, the exponent l in eqn. (3) is always negative for the wetting curve and positive for the drying curve.

Relatively large differences also exist between K_s values for the wetting and drying curves. Because the gradient $dK/d\theta$ can be very large near saturation in the model of van Genuchten (1980), K_s is used as a scale parameter to match the predicted and measured hydraulic conductivity curves. Therefore, the fitted parameter values of K_s in Table 3 may deviate considerably from the actually measured values in Fig. 4. These differences in K_s have little effect on the calculated water and solute distributions because of the relatively small

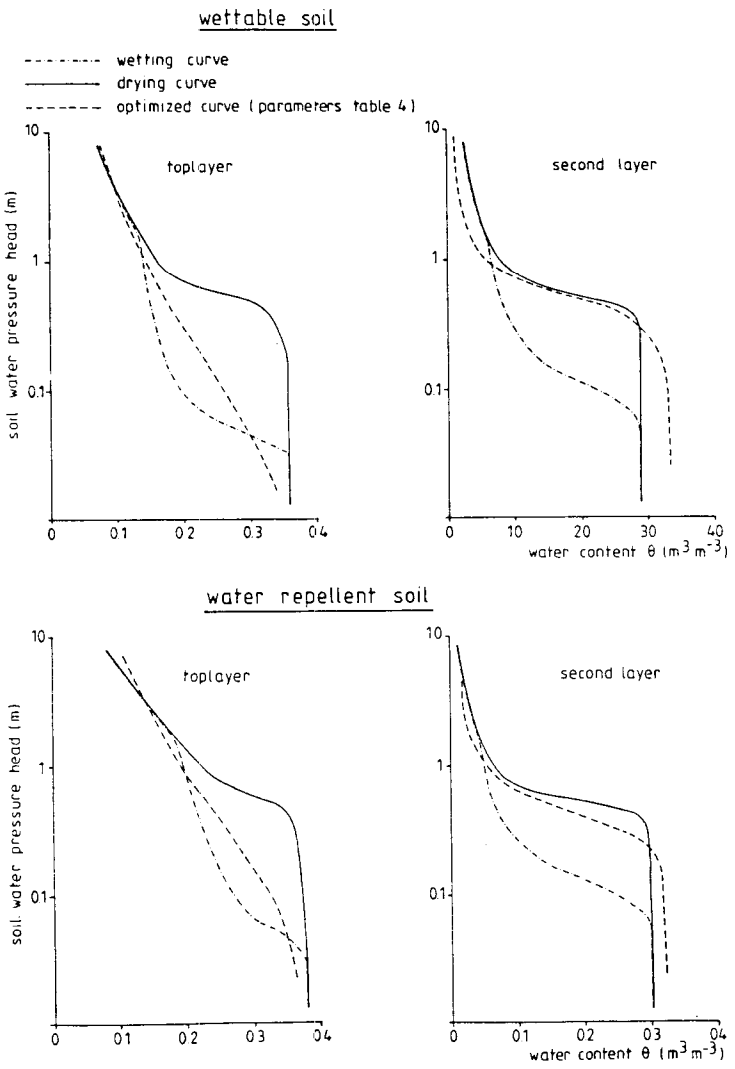

Fig. 3. Water retention curves of the wettable and water-repellent soils.

water flow rates during the experiments (the surface layers always remained unsaturated). Figure 4 shows that, except for the region near saturation, the measured and fitted hydraulic conductivity curves agree reasonably well.

Unsaturated flow experiments

First, the unsaturated water flow was simulated using the optimized hydraulic parameters given in Table 3. This effort did not yield satisfactory results as reflected by rather low relative efficiencies (RE = 50.9 resp.

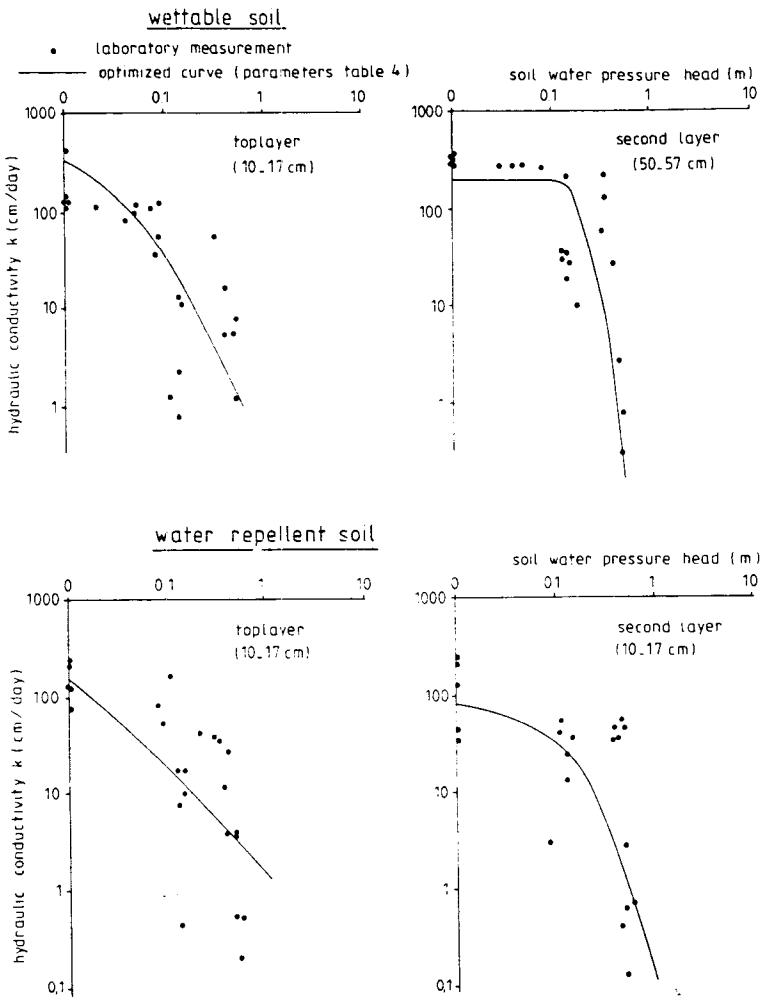

Fig. 4. Hydraulic conductivity curves of wettable and water-repellent soils.

– 112.7%). To improve the predictions we estimated the water retention curves directly from the field-measured water content distributions using an inverse procedure. Inverse methods have been used successfully in previous studies, including those by Dane and Hruska (1983) and Kool et al. (1987), to determine the water retention and hydraulic conductivity functions from transient flow data. In the inverse problem we minimized the objective function O(**b**)

$$0(\mathbf{b}) = \sum_{i=1}^{p} [\theta_i^* - \theta_i(\mathbf{b})]^2 \tag{14}$$

where θ_i^* are the p measured water contents at selected times and depths, and

TABLE 3

Parameters of the laboratory-measured unsaturated soil hydraulic functions

	Wettable soil				Water-repellent soil			
	Top layer		Second layer		Top layer		Second layer	
Parameter	Wet	Dry	Wet	Dry	Wet	Dry	Wet	Dry
θ_r (-)	0.01	0.01	0.01	0.02	0.01	0.01	0.01	0.02
θ_s (-)	0.38	0.38	0.30	0.30	0.38	0.38	0.30	0.30
α (m^{-1})	25.00	1.0	5.00	1.30	38.00	1.80	21.00	2.90
n (-)	1.3	1.9	2.0	7.0	1.3	1.9	1.7	2.3
l (-)	-3.0	0.5	-0.5	2.0	-4.0	2.0	-3.0	2.0
K_s (m day^{-1})	17.0	1.5	3.0	1.0	15.0	1.6	3.0	3.0

Wet = wetting curve; dry = drying curve.

$\theta_i(\mathbf{b})$ are the corresponding water contents predicted with the numerical model using the vector of unknown parameters $\mathbf{b} = \{\theta_r, \theta_s, \alpha, n, l, K_s\}$. The parameters of the measured wetting and drying curves were used as upper and lower limits by the optimization procedure. The parameters α, n, l and K_s were kept variable; θ_r was assumed to be zero for this soil and θ_s was kept on its measured values.

For the minimization of $O(\mathbf{b})$ several methods can be used (Jacoby et al., 1972). We used the 'direct search' method of Hooke and Jeeves (1961), which requires no derivatives and is easy to program. The method assumes a unimodal function; therefore, if more than one minimum exists or the shape of the function-surface is unknown, several sets of starting values are necessary to find the absolute minimum. In the algorithm $O(\mathbf{b})$ is evaluated around sets of parameters (base points). For each parameter side steps are made. If $O(\mathbf{b})$ decreases a new base point is determined. When $O(\mathbf{b})$ only increases the side steps are reduced and searches are made around the latest best point. It may be clear from this that the computing time increases considerably when more variables have to be optimized simultaneously or when evaluation of $O(\mathbf{b})$ requires many operations.

Results of the parameter estimation process are listed in Table 4. This table also includes estimates for the hydraulic parameters of a third soil layer consisting of mostly sandy material with locally thin allochthonously eroded, disintegrated peat layers (Hendrickx et al. 1988b). This third layer causes the relatively high water contents at a depth of 0.65–0.85 m (see water contents on 12 November 1986 in Fig. 1). Figure 5 compares the measured and calculated water contents using the field-estimated hydraulic parameters. The relative efficiencies are now acceptable: 81.7 and 89.1% for the wettable and water-repellent soils, respectively (Table 5). This suggests that water flow is adequately simulated during the bromide tracer experiment.

TABLE 4

Optimized values for the field-measured soil hydraulic and solute transport parameters

	Wettable soil			Water-repellent soil		
Depth (m)	0–0.30	0.30–0.67	0.67–0.83	0–0.32	0.32–0.65	0.65–0.83
Hydraulic parameters						
θ_r (-)	0.01	0.02	0.02	0.01	0.01	0.04
θ_s (-)	0.38	0.32	0.40	0.36	0.33	0.40
α (m^{-1})	10.00	2.50	5.00	27.00	2.20	5.00
n (-)	1.3	4.0	2.8	1.3	3.5	3.0
l (-)	−1.0	2.0	−1.0	−5.0	0.5	−1.0
K_s ($m\,day^{-1}$)	15.0	1.0	3.0	10.0	0.8	1.0
Transport parameters						
λ (m)	0.02	0.02	0.02	0.03	0.03	0.03
F (-)	0.85	1.0	1.0	0.7	0.8	1.0

Bromide transport experiments

After modelling the water flow, the solute parameters λ and F were estimated. The parameter F has a relatively strong effect on the position of the solute front (Fig. 6) but hardly influences the simulated water contents due to the low rain intensity. For this reason F could be optimized after the soil hydraulic properties were fixed.

The measurements revealed relatively high bromide concentrations in the upper 10 cm of the profile during the entire experiment, especially for the water-repellent soil (Fig. 2). We attribute this to delayed transport of bromide that was sprayed above stagnant (non-wettable) parts. We could not justify an impulse input and had to account somehow for the very slow release of bromide from the non-wettable to the wettable part of the surface soil. The gradual release was accounted for by using a linear adsorption isoterm for the top 5 cm of the water repellent soil (eqn. (7)). Although in reality the process causing gradual release is complex and difficult to quantify, the linear adsorption coefficient can be used to macroscopically account for the retardation of the solute in the top soil. Adsorption causes the bromide distribution to become skewed with a gentle slope at the upper side (Fig. 7).

The second and third field bromide sampling, showed concentration distributions at each depth; these were often skewed with a few high concentrations. Because Shapiro–Wilk tests revealed that these skewed distributions were generally neither normally nor lognormally distributed, we decided to use the median concentration per depth for parameter optimization.

Table 4 lists the optimized transport parameters. The dispersivity λ for the wettable soil is 0.02 m and for the water-repellent soil 0.03 m, which is relatively low for field soils (e.g. Biggar and Nielsen, 1976; Jury and Sposito, 1985; van Ommen, 1989a). F was estimated to be 0.85 for the wettable top layer, which was

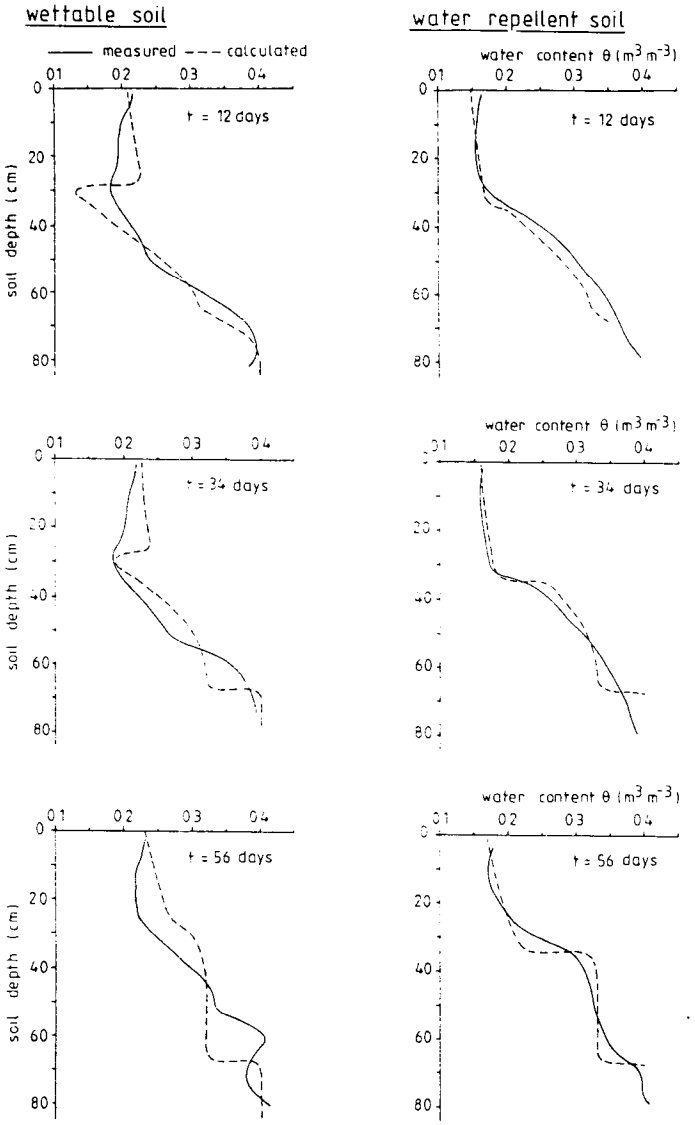

Fig. 5. Comparison of measured and simulated soil water contents. Calculated curves were obtained with the optimized parameters in Table 4.

TABLE 5

Relative efficiencies *RE*% for simulation of water content

	Wettable soil	Water-repellent soil
Wetting curve	26.4	− 68.9
Drying curve	− 10.2	15.6
optimization	81.7	89.1

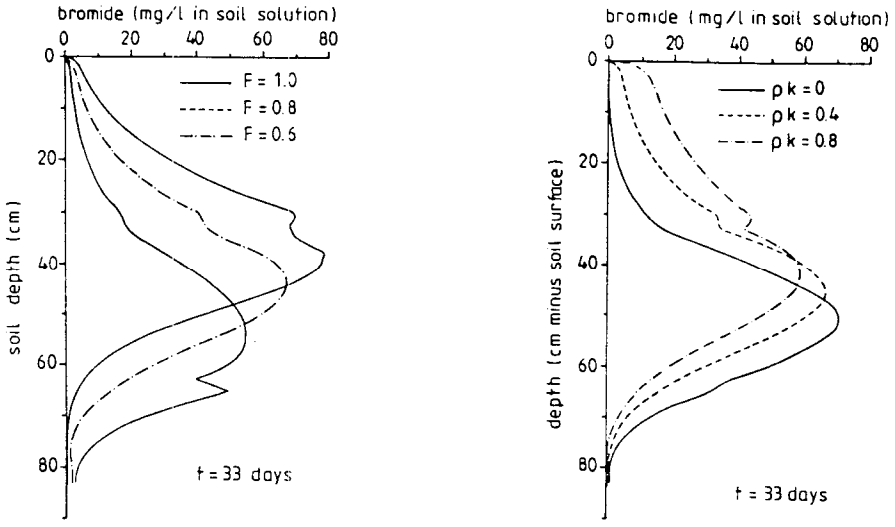

Fig. 6. Effect of stagnant parts in the top and second layer on simulated bromide concentrations, in the water-repellent soil.

Fig. 7. Effect of adsorption in the upper 5 cm on simulated bromide concentrations, in the water-repellent soil.

contrary to our expectations. A value for F of less than unity may be caused by some slight water-repellency of the top layer (Hendrickx et al., 1988b).

Figure 8 shows a close fit between measured and calculated bromide concentrations, especially after 34 days. The rather good fit is also reflected by the relatively high RE values (82 and 80%) for the two soil conditions. The observed solute front in the water-repellent soil at $t = 55$ days stays behind the calculated front. We believe that this is caused by horizontal flow induced by thin less-permeable peat lenses at 60–90 cm below the soil surface.

SENSITIVITY OF THE MODEL

The sensitivity of the numerical model was tested by simulating the field experiments in the water-repellent soil using deviating parameter values and boundary conditions. The following cases were considered: (1) the use of wetting and drying curves; (2) changes in soil layering; (3) steady state vs. transient flow; (4) pulse input vs. gradual release; (5) variations in the saturated hydraulic conductivity, K_s.

The relative efficiency RE for each simulation is listed in Table 6. Results are given using both the median and the mean of the measured bromide concentrations at each depth. The simulations were compared with the mean of 13 observations (excluding two deviating soil columns), and with the mean of all observations ($N = 15$). Relative efficiencies derived from mean concentrations are generally lower than those stemming from measured median values

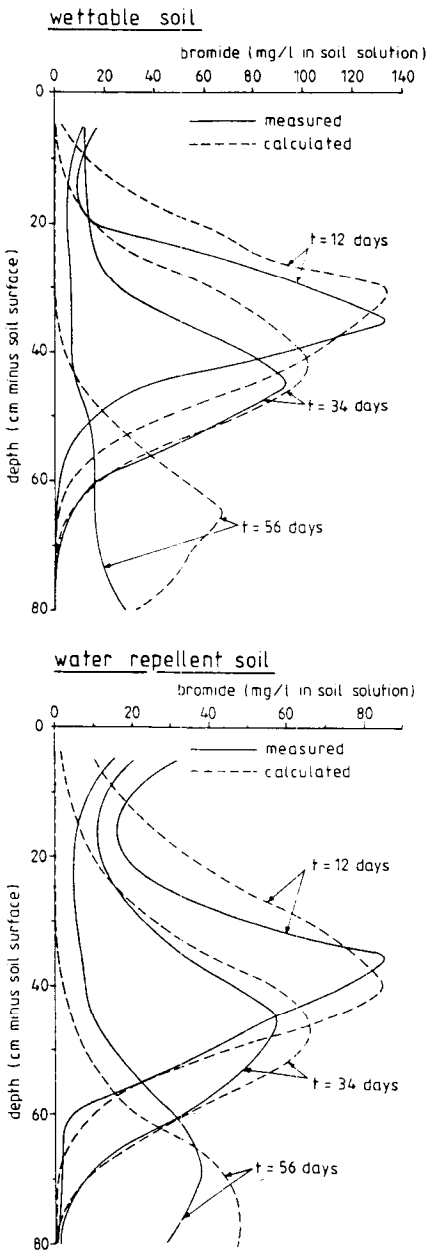

Fig. 8. Comparison of simulated and measured bromide concentrations.

suggesting that the "average" behaviour of a water-repellent soil (as described by the median) can be predicted quite well with the model. The sensitivities for each of the above five cases are briefly discussed below.

TABLE 6

Relative efficiencies, RE, for selected simulations using both the median and the mean of the measured bromide concentrations

	Wettable soil		Water-repellent soil			
	Median (N = 15)	Mean (N = 15)		Median (N = 15)	Mean (N = 13)	Mean (N = 15)
F = 1.00	48.3	50.9	F = 1.00	− 112.7	− 91.8	− 196.8
F = 0.85	72.3	79.9	Field-optimization	82.1	89.0	57.8
F = 0.70	63.1	77.8	Wetting curve	− 136.2	− 70.8	− 110.0
			Drying curve	46.1	44.4	− 2.0
			Homogeneous profile	57.8	75.9	34.3
			Steady-state flow	76.8	85.8	56.8
			Impulse input	50.5	72.0	33.7
			K_s decreased	74.2	75.9	41.1

The use of wetting and drying curves

Initially it seemed reasonable to use in the simulations the wetting curve as measured in the laboratory. However, the low RE (− 136.2%) for this case indicated that the laboratory-measured wetting curve did not perform well. The drying curve performed somewhat better by yielding an RE of 46.1% vs. the median. However, both curves measured in the laboratory yielded inferior results as compared with the soil water retention curves estimated directly from field-measured soil water contents, using the inverse method (RE = 82.1%).

Changes in soil layering

The hydraulic parameters of the top and the second layer are quite different (Table 4). If the hydraulic and transport parameters of the top soil were assumed to be equal to those of the second layer, the bromide pulse would move much faster in the upper part of the profile because of the lower water contents in the first layer. This change causes a reduction in the relative efficiency from 82.1 to 57.8%. Thus the soil morphological distinction between top and second layer (Hendrickx et al., 1988a) is physically meaningful.

Steady-state vs. transient flow conditions

The numerical code used for this study (WORM) allows fluxes or potentials at the upper and lower boundary of the soil column to be time-dependent. When the experiments were simulated with the constant rainfall and groundwater depth, the efficiency of the simulation still equalled 76.8%. The difference in simulated bromide concentrations between steady state and transient-flow conditions was very small for our experiment. This is consistent with the study

of Wierenga (1977) who found that the quality of drainage water during intermittent irrigation was predicted equally well when using a steady-state or a transient water flow model.

Impulse input vs. gradual release

Neglecting the gradual delivery of the bromide from the top soil (simulated by introducing an adsorption coefficient in the first 5 cm) resulted in a decrease of the RE from 82.1 to 50.5%. The pulse propagated faster while the spreading of the solute was less. Gradual delivery and stagnant parts have opposite effects on the bromide concentrations (Figs. 6 and 7). Simulation with $F = 0.85$, no adsorption and dispersivity $\lambda = 0.05$, yielded an RE as high as 79.6%. However, in this way λ not only accounted for the effects of molecular diffusion and mechanical dispersion but also for dispersion caused by stagnant parts and delayed transport of bromide. The dispersivity increased from 0.03 to 0.05 m. If the intention is to restrict dispersivity to molecular diffusion and mechanical dispersion and to give a realistic estimation of the stagnant parts, it is necessary to incorporate adsorption in the upper layer.

Effect of preferential flow paths

Calculated water contents increased with decreasing factor F, but the differences were very small. The relatively low rain intensities during winter caused the soil water pressure to be mainly determined by the distance to the groundwater table. The location of the maximum bromide concentration was approximately inversely proportional to F (Fig. 6). Simulation of the water-repellent soil with $F = 1.00$ resulted in a very low RE ($-$ 112.7%). Table 6 also shows for the wettable soil the RE with and without accounting for preferential flow. Apparently some preferential flow ($F = 0.85$) did occur.

Variations in the saturated hydraulic conductivity

Estimated values for the saturated hydraulic conductivity, K_s vary considerably (e.g., Table 4). Reducing K_s caused the calculated water potentials to become higher, the differences being largest in the surface soils. The pore water velocity also became less as the water content increased but the water fluxes (as determined for the rainfall rates) remained identical. The influence of K_s on the calculated bromide concentrations was found to be relatively small; reduction of K_s by a factor of 10 resulted in an RE of 74.2%. These simulations suggest that accurate measurement of K_s may not always be a prerequisite for correctly simulating solute transport in the vadose zone.

SUMMARY AND CONCLUSIONS

Observed water content and bromide concentration distributions in a water-repellent unsaturated soil profile were compared with results obtained with a

numerical program. Water and bromide transport during the unstable flow conditions could be predicted well with a relatively simple model which adjusts the soil water content and unsaturated hydraulic conductivity to the volume fraction of soil occupied by preferential flow paths. Field observations were not satisfactorily described when soil hydraulic properties were used that were determined in the laboratory. Results improved considerably when the laboratory-measured curves were used in combination with an inverse optimization method. Further refinements were obtained when an adsorption coefficient was introduced for the top 5 cm of soil to account for a retarded bromide release from the water-repellent top soil.

ACKNOWLEDGMENT

The authors wish to thank W. Hamminga, P.B.J.M. Oude Boerrigter and J.P.M. Burger for their field and laboratory work.

REFERENCES

Albert, R. and Köhn M., 1926. Untersuchungen uber den Benetzungswiderstand von Sandboden. Mitt. Int. Bodenkd. Ges., 2: 146–153.

Biggar, J.W. and Nielsen, D.R., 1976. Spatial variability of the leaching characteristics of a field soil. Water Resour. Res., 12: 78–84.

Bolt, G.H., 1982. Soil Chemistry: B. Physico-chemical Models. Elsevier, Amsterdam, 2nd edn., pp. 285–348.

Dane, J.H. and Hruska S., 1983. In-situ determination of soil hydraulic properties during drainage. Soil Sci. Soc. Am. J., 47: 619–624.

De Bakker, H., 1979. Major soils and soil regions in The Netherlands. Junk, den Haag and Pudoc, Wageningen, 203 pp.

DeBano, L.F., 1969. Water repellent soils: a worldwide concern in management of soil and vegetation. Agric. Sci. Rev., 7: 11–18.

DeBano, L.F., 1975. Infiltration, evaporation and water movement as related to water repellency. Soil Sci. Soc. Am., Spec. Publ., 7, pp. 155–163.

DeBano, L.F., 1981. Water repellent soils: a state-of-the-art. Pacific Southwest For. Range Exp. Stn. Gen. Tech. Rep. PSW-46, 21 pp.

De Smedt, F. and Wieringa, P.J., 1979. Mass transfer in porous media with immobile water. J. Hydrol., 41: 59–67.

Diment, G.A. and Watson K.K., 1983. Stability analysis of water movement in unsaturated porous materials: 2. Numerical studies. Water Resour. Res., 19: 1002–1010.

Diment, G.A. and Watson, K.K., 1985. Stability analysis of water movement in unsaturated porous materials: 3. Experimental studies. Water Resour. Res., 21: 979–984.

Diment, G.A., Watson K.K. and Blennerhassett, P.J., 1982. Stability analysis of water movement in unsaturated porous materials: 1. Theoretical considerations. Water Resour. Res., 18: 1248–1254.

Germann, P.F., 1988. Approaches to rapid and far-reaching hydrologic processes in the vadose zone. In: P.F. Germann (Editor), Rapid and Far-reaching Hydrologic Processes in the Vadose Zone. J. Contam. Hydrol., 3: 115–127.

Glass, R.J., Steenhuis, T.S. and Parlange, J-Y., 1988. Wetting front instability as a rapid and far-reaching hydrologic process in the vadose zone. In: P.F. Germann (Editor), Rapid and Far-reaching Hydrologic Processes in the Vadose Zone. J. Contam. Hydrol., 3: 207–226.

Harmsen, J., 1986. Optimalisation of column choice, eluent preparation and detection by ion chromatography of inorganic anions. Nota 1699, ILRI, Wageningen, 46 pp.

Hendrickx, J.M.H., Dekker L.W., Bannink M.H. and van Ommen, H.C., 1988a. Significance of soil survey for agrohydrological studies. Agric. Water Manage., 14: 195–208.

Hendrickx, J.M.H., Dekker, L.W., van Zuilen, E.J. and Boersma O.H., 1988b. Water and solute movement through a water repellent sand soil with grass cover. Proceedings of a Conference on the Validation of Flow and Transport Models for the Unsaturated Zone, Ruidoso, New Mexico, pp. 131–146.

Hill, E.D. and Parlange, J.Y., 1972. Wetting front instability in layered soils. Soil Sci. Soc. Am. Proc., 36: 697–702.

Hillel, D., 1987. Unstable flow in layered soils: a review. Hydrol. Proc., 1: 143–147.

Hooke, R. and Jeeves, T.A., 1961. Direct search solution of numerical and statistical problems. J. Assoc. Comp. Mach., 8: 212–229.

Jacoby, S.L.S., Kowalik J.S. and Pizzo, J.T., 1972. Iterative methods for nonlinear optimization problems. Prentice-Hall, Englewood Cliffs, NJ.

Jamison, V.C., 1945. The penetration of irrigation and rain water into sandy soils of central Florida. Soil Sci. Soc. Am. Proc., 10: 25–29.

Jury, W., 1982. Simulation of solute transport using a transfer function model. Water Resour. Res., 18(2): 363–368.

Jury, W.A. and Sposito, G., 1985. Field calibration and validation of solute transport models for the unsaturated zone. Soil Sci. Soc. Am. J., 49: 1331–1341.

Kool, J.B., Parker J.C. and van Genuchten, M.Th., 1987. Parameter estimation for unsaturated flow and transport models — a review. J. Hydrol., 91: 255–293.

Letey, J., Osborn, J.F. and Valoras, N., 1975. Soil water repellency and the use of nonionic surfactants. Calif. Water Res. Center, Contrib. 154.

McCuen, R.H. and Snyder, W.M., 1986. Hydrologic modeling. Statistical methods and applications. Prentice-Hall, Englewood Cliffs, NJ.

McGhie, D.A. and Posner, A.M., 1980. Water repellency of a heavy-textured Western Australia surface soil. Aust. J. Soil Res., 18: 309–323.

Meeuwig, R.O., 1971. Infiltration and water repellency in granitic soils. USDA For. Serv. Res. Pap. INT-111, Ogden, UT 84401, 20 pp.

Mualem, Y., 1976. A new model for predicting the hydraulic conductivity of unsaturated media. Water Resour. Res., 12: 513–522.

Parlange, J.Y. and Hill, D.E., 1976. Theoretical analysis of wetting front instability in soils. Soil Sci., 122: 236–239.

Philip, J.R., 1975. Stability analysis of infiltration. Soil Sci. Soc. Am. J., 39: 1042–1049.

Raats, P.A.C., 1973. Unstable wetting fronts in uniform and nonuniform soils. Soil Sci. Soc. Am. J., 37: 681–685.

Richardson, J.L., 1984. Field observation and measurement of water repellency for soil surveyors. Soil Surv. Horizons, 25: 32–36.

Starr, J.L., DeRoo, H.C., Frink, C.R. and Parlange, J.Y., 1978. Leaching characteristics of a layered field soil. Soil Sci. Soc. Am. J., 42: 386–391.

Van Genuchten, M.Th., 1980. A closed form equation for predicting the hydraulic conductivity of unsaturated soils. Soil. Sci. Soc. Am. J., 44: 892–898.

Van Genuchten, M.Th., 1982. A comparison of numerical solutions of one-dimensional unsaturated-saturated flow and mass transport equations. Adv. Water Resour., 5: 47–55.

Van Genuchten, M.Th., 1987. A numerical model for water and solute movement in and below the root zone. Unpubl. Res. Rep. (121), USDA ARS, U.S. Salinity Laboratory, Riverside, CA.

Van Ommen, H.C., Dijksma, R., Hendrickx, J.M.H., Dekker, L.W., Hulshof, J. and van den Heuvel, M., 1989a. Experimental and theoretical analysis of solute transport from a diffuse source of pollution. J. Hydrol., 105: 225–251.

Van Ommen, H.C., van Genuchten, M.Th., van der Molen, W.H., Dijksma, R. and Hulshof, J., 1989b. Experimental assessment of preferential flow paths in a field soil. J. Hydrol., 105: 253–262.